Rock Mechanics and Rock Engineering
https://doi.org/10.1007/s00603-018-1443-z

TECHNICAL NOTE

Static and Dynamic Response of Bakken Cores to Cyclic Hydrostatic Loading

Xiaodong Ma[1,2,3] · **Mark D. Zoback**[1]

Received: 20 December 2016 / Accepted: 20 February 2018

Keywords Bakken · Hydrostatic compression · Hysteresis · Pressure-dependency · Seasoning · Tight reservoir rocks

1 Introduction

It has been acknowledged that the cores extracted from underground are not always fully representative of the in situ material (e.g., Santarelli and Dusseault 1991; Warpinski and Teufel 1992; Ewy 2015). Even with careful handling and storage, the mechanical properties of the cores are inevitably altered due to stress relief, drainage and cooling, exposure to air or other fluids, etc. These effects can introduce irreversible changes to most rocks, which have been observed in terms of rocks' permeability, deformability, and velocities (Bernabé 1986; Wang and Simmons 1978; Warpinski and Teufel 1992). Depending on the degree of alteration, the laboratory measurements of the cores may be highly variable and sporadic. Since it affects the attempts to correlate the laboratory results to in situ conditions, it is imperative to evaluate and to minimize the laboratory measurement reproducibility.

In the laboratory, the evolution of the measured core properties is often observed when the core is subject to repeated, hydrostatic loading–unloading cycles (Bernabé 1986; Warpinski and Teufel 1992). This evolution is likely to diminish within a number of cycles, and then the measurements are deemed reproducible and reliable. This cycling procedure is often called 'seasoning.' Different from other cyclic tests (Haimson 1974; Zoback and Byerlee 1975), seasoning typically subjects the specimen to hydrostatic confining stress and controls the stress between zero and a predetermined maximum level. The notion of seasoning was coined by Bernabé (1986), who suggested that the seasoning process could close some of the microcracks and may presumably yield a non-variable material. Warpinski and Teufel (1992) adopted the seasoning procedure in testing a few tight reservoir rocks and showed the seasoning significantly reduces uncertainties. Boutéca et al. (1998) claimed seasoning led to intrinsic properties of a porous, quartz-rich sandstone. However, Ostermeier (1995) argued seasoning could not improve reproducibility based on their tests on the Gulf of Mexico turbidites. They emphasized that for a viscoelastic material, seasoning may never be achieved. Apparently, the influence of seasoning on the evolution of mechanical properties varies significantly between different rocks.

In this study, we seasoned five cores associated with the Bakken tight oil play. Specifically, the objective of seasoning process was twofold: (1) to characterize the evolution of mechanical response of these rocks over pressure cycles and (2) to understand the effectiveness of seasoning on leading to reproducible measurements. During seasoning, we monitored both the static and dynamic responses (deformation and ultrasonic velocities) over multiple cycles until the discrepancy between cycles substantially diminished. Then, the dependency on confinement, loading–unloading hysteresis, and evolution between cycles were examined.

✉ Xiaodong Ma
xiaodongma.rocks@gmail.com

Mark D. Zoback
zoback@stanford.edu

[1] Department of Geophysics, Stanford University, 397 Panama Mall, Stanford, CA 94305, USA

[2] State Key Laboratory of Geomechanics and Geotechnical Engineering, Institute of Rock and Soil Mechanics, Chinese Academy of Sciences, Wuhan 430071, China

[3] Present Address: Swiss Competence Center for Energy Research (SCCER-SoE), and Chair for Geothermal Energy and Geofluids, ETH Zürich, Zürich 8092, Switzerland

Published online: 07 March 2018

2 Materials and methods

The Bakken cores used in this study were extracted from a vertical well at depths between 3017.52 and 3124.2 m. This depth range covers the primary sequences of the Lodgepole, Middle Bakken, and Three Forks. A total of five bedding-perpendicular (vertical, as denoted with 'V' in sample IDs) cores sampling these sequences are available. Details regarding the mineral composition, petrographic classification, and physical properties of these cores are listed in Table 1.

The mineral composition of these core samples varies unpredictably between carbonate-rich to silicate-rich, representative of these mixed carbonate–silicate sequences. The relative abundance of carbonate and silicate sediments dictates the microstructures of these core samples. Figure 1 shows the distinct microstructures of the pristine cores. A detailed microscopic description and micromechanical observation were documented by Ma and Zoback (2017).

According to Yang and Zoback (2014), the drilled well has a stress gradient of $S_{Hmax}/S_{hmin}/S_V = \sim 23.8/21.5/18.1$ MPa/km. This results in a mean stress S [$=(S_{Hmax}+S_{hmin}+S_v)/3$] of nearly 65 MPa at the depth of ~ 3 km where the cores were obtained. To replicate the possible in situ stress magnitude, we set our maximum confining pressure (P_c) at 70 MPa for all five Bakken cores.

The core samples used in this study had been exposed to room-temperature, room-dry environment for an extended period of time (~ 3 years), so we expect that stress relief, desiccation, and cooling may have gradually altered them (Dewhurst and Siggins 2006; Sarout and Guéguen 2008; Josh et al. 2012; Ewy 2015; Dewhurst et al. 2015) to the degree which can be difficult to quantify. Without attempts to restore them to their pristine confined, ambient and

Table 1 Summary of tested specimens (modified from Ma and Zoback 2017)

Sample ID	Rock type	Mineral composition (wt%)			Porosity (%)	Depth (m)	Estimated in situ[a] S (P_P) (MPa)
		QFM[b]	Carbonates	Clays			
B1V	Lime wackestone	0.08	0.87	0.05	3.67	3022.1	65.0 (43.5)
B3V	Fine sandstone	0.58	0.31	0.11	7.12	3037.9	65.3 (43.7)
B4V	Lime packstone	0.30	0.47	0.22	10.1	3064.6	65.9 (47.2)
B9V	Fine sandstone	0.70	0.19	0.10	3.06	3069.4	66.0 (47.2)
B10V	Dolomite sediment	0.31	0.51	0.15	14.35	3123.6	67.1 (48)

[a] S, means in situ stress; P_p, pore pressure. Estimation based on Yang and Zoback (2014)

[b] QFM: Quartz, feldspar, and mica

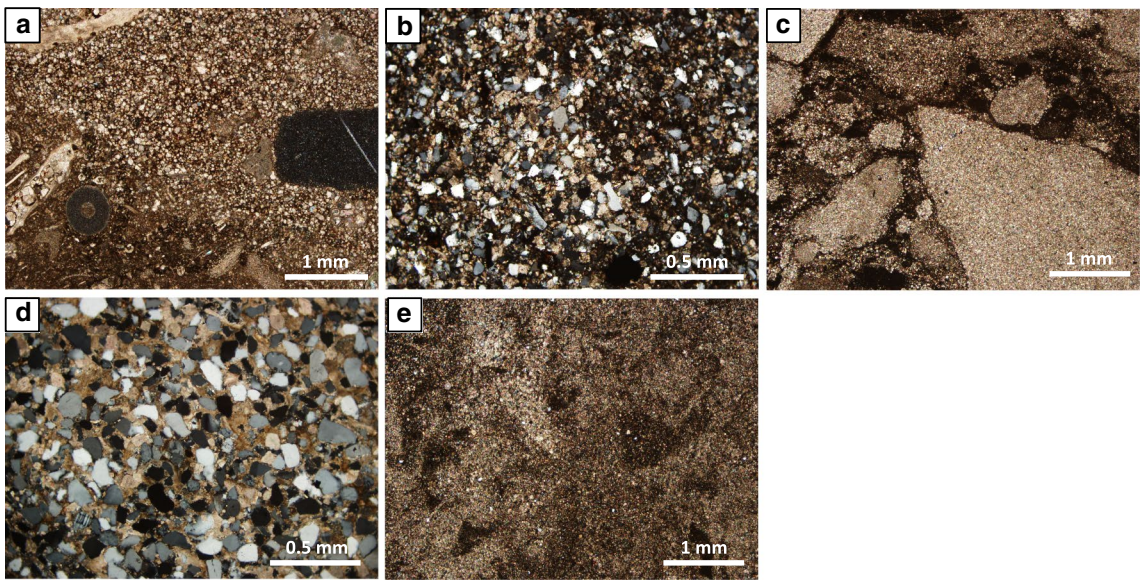

Fig. 1 Thin-section photomicrographs (cross-polarized light) of five Bakken cores prior to testing. Thin-sections are oriented perpendicular to core axes. **a** B1V, **b** B3V, **c** B4V, **d** B9V, and **e** B10V

hydrous condition in situ, all cores were handled and tested 'as is.' Retrospectively, it is difficult to track and estimate the loss of pore fluid content and the associated volume change over time from the original in situ condition. Restoration process is considered impractical in these low-permeability rocks and would likely introduce other unfavorable effects, such as swelling of clay particles, reorganization of grain contacts, and incurring visco- and/or plastic-response (e.g., Pham et al. 2005; Sarout et al. 2014). Furthermore, the removal of fluid content by oven-drying was not executed in order to best preserve the original hydration states of the clay minerals (for details on water removal via oven-drying, see Sarout and Guéguen (2008)).

The remaining fluid content (although not necessarily saturated) can cause poroelastic effects when the core is loaded under high confinement. The poroelastic effect can be minimized with improved sample permeability and increased time for pore pressure dissipation. To this end, we drilled three evenly spaced but misaligned boreholes (8.5 mm depth and 1 mm diameter) on each end of the specimen (Fig. 2) to increase sample permeability (see Ma and Zoback (2017) for technical details). Stainless-steel porous disks were also placed between specimen and core holder to provide void space for any fluid volume to drain out (and open to vacuum) when specimen is highly compressed. Although the loading/unloading stress steps were applied almost instantaneously, we wait sufficiently long time (usually 2–3 h) between each step to allow the pore pressure build-up to sufficiently dissipate. Equilibrium was deemed achieved when the strain readings eventually stabilized.

The cores were prepared into cylindrical specimens of 25.4 mm length and 25.4 mm diameter, with both ends grounded flat and parallel and the specimen axis perpendicular to bedding planes. The specimen was then jacketed and sandwiched by two core holders, and put inside a conventional triaxial vessel (Ma and Zoback 2016a, b). During the test, servo-controlled hydraulic system subjected the specimen to hydrostatic confining pressure (P_c) under fully drained conditions. The specimen underwent the so-called seasoning procedure (Bernabé 1986; Warpinski and

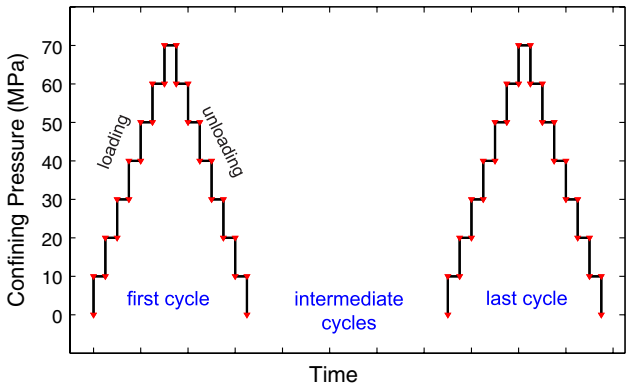

Fig. 3 Loading path of seasoning cycles. The loading/unloading step is instantaneous and followed by sufficient time for mechanical equilibrium. Each red symbol represents one measurement

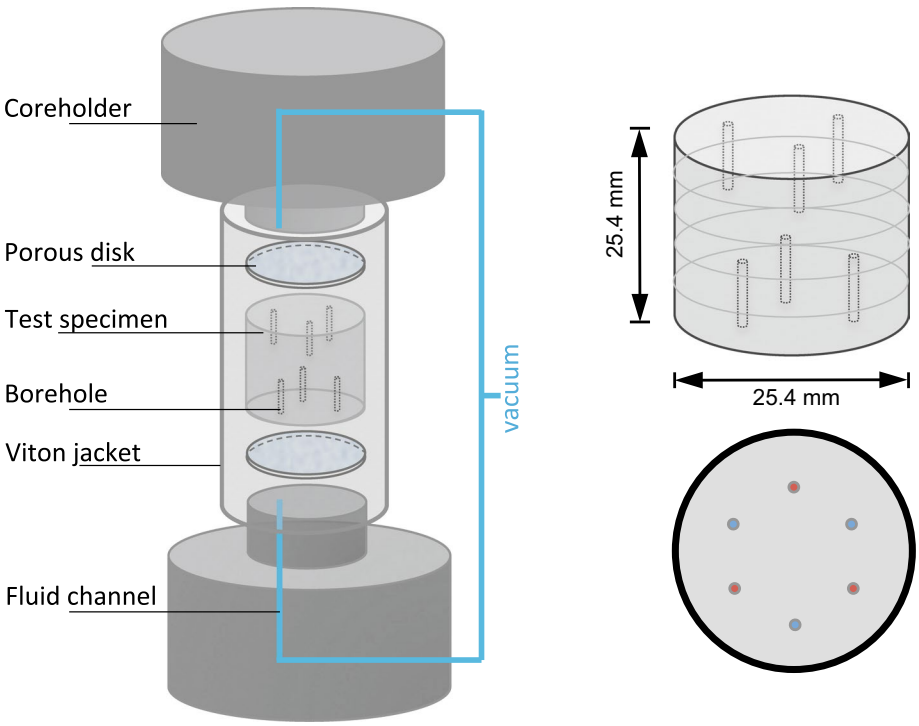

Fig. 2 Left: illustration of the experimental specimen-coreholder assembly housed inside a pressure vessel. Right: dimensions of the specimen and the configuration of boreholes drilled inside the specimen

Teufel 1992), in which the load was cycled between zero and maximum stress multiple times (Fig. 3). All specimens were typically cycled three times, although only the first and last cycles were recorded for most specimens. The seasoning is considered as a preconditioning process for reproducibility of subsequent experiments on poroelasticity (Ma and Zoback 2017).

Two pairs of electrical-resistance strain gages were epoxied directly on the specimen surface to measure its axial and circumferential deformations. Ultrasonic velocities (*P*- and *S*-waves) along the axial direction were measured using a coupled wave emitter and receiver embedded in the upper and lower core holders, respectively. The uncertainty of velocity measurements mainly comes from the low length-to-width ratio of the specimen (1:1) but will be limited since the frequency piezoelectric crystals are at 1 MHz. Considering the crystals attachment to the titanium transducer and the rock sample in this study, the center frequency of the measurements is estimated to be around 750 kHz (*New England Research*, personal communication). Considering the sources of uncertainty caused by arrival time picks and sample length measurements, the velocity measurement error is of the order of 2% (for details of error analysis, see Hornby (1998), Dewhurst and Siggins (2006), and Sarout and Guéguen (2008)).

3 Test Results

3.1 Deformation Data

The principal strains ε_{ax} and ε_{lt} of the specimen were recorded along the axial and circumferential (lateral) directions, respectively. For cylindrical bedding-perpendicular specimen, volumetric strain (ε_{vol}) of the specimen was simply calculated via $\varepsilon_{vol}=\varepsilon_{ax}+2\varepsilon_{lt}$, in view of their transversely isotropy (Ma and Zoback 2017). Each specimen's principal and volumetric strains are shown in Fig. 4 for the first and final loading cycles applied. The data are displayed in terms of confining stress versus strain, so that the local tangent to the stress–strain curve is readily a measure of the rock stiffness. In general, the rock stiffness increases consistently with confining pressure, although the degree of stiffening highly varies between specimens. For each loading and unloading cycle, the trend can be adequately fitted by a second-order polynomial equation (Fig. 4). The stiffening of these specimens with P_c is considered as a result of microcracks/pores closure and/or the compaction of compliant material (mainly clays and kerogen) (e.g., Vernik and Liu 1997; Sone and Zoback 2013).

For all specimens, the axial deformation is unequivocally greater than the lateral deformation at any given stress level. And the axial strain is more sensitive (greater curvature in the stress–strain relationship) to confining pressure than the lateral strain. Although the stress–strain response along each principal direction under hydrostatic loading simply is not characteristic of the *Young*'s modulus in that direction (which is typically characterized under uniaxial loading), the observed difference between the axial and lateral deformation reflects the rock's deformational anisotropy. This static deformational anisotropy is expected in these sedimentary rocks considering the preferred alignment of compliant components (clay minerals or organic contents, or in the form of stress-relief microcracks) with beddings (Vernik and Liu 1992, 1997; Hornby et al. 1994; Johnston and Christensen 1995; Sondergeld et al. 2000; Sondergeld and Rai 2011; Vernik and Milovack 2011).

Hysteresis between loading and unloading within one cycle persists in all five specimens (Fig. 4). Typically, strain along the unloading curve is smaller than along the previous loading curve. It is true in both axial and lateral strains. We also noticed the hysteresis in the axial direction is significantly greater than in the lateral direction, and it appears that the hysteresis in the volumetric strain should be mainly attributed to that in the axial direction.

As the specimen undergoes multiple cycles of loading and unloading, it is evident that subsequent cycles induce additional inelastic compaction; however, the inelastic compaction caused by each cycle gradually diminishes with the number of runs (Fig. 4). For convenience and clarity, we only display the first and final cycles in these five specimens.

3.2 Ultrasonic Velocities

Ultrasonic velocities, *V*p and *V*s, in the axial direction were calculated based on *P*- and *S*-wave travel times, respectively. The relationship between velocities and confining pressure is presented in Fig. 5. Both *V*p and *V*s increase with confining pressure, albeit the rate of increase rapidly slows down with the rise of confining pressure. Taking the first loading cycle of all Bakken cores as an example, the first 10 MPa confinement generally contributes to nearly half of the total velocity increase and then the rate of increase drops significantly for the additional 60 MPa of confinement toward the maximum load.

Although the scatter in velocity data is somewhat higher than the deformation data, especially under low confinement, a general discrepancy between cycles is still measurable. During the first unloading cycle, both *V*p and *V*s are higher than the first loading cycle at the same magnitude of confining pressure (Fig. 5). In the final loading cycle, both *V*p and *V*s at all stress levels are higher than their counterparts in the first loading cycle, but slightly less than those in the first unloading cycle when confining pressure is approximately below 20 MPa. (Then the two became nearly the same for higher confining pressure.) This is best illustrated

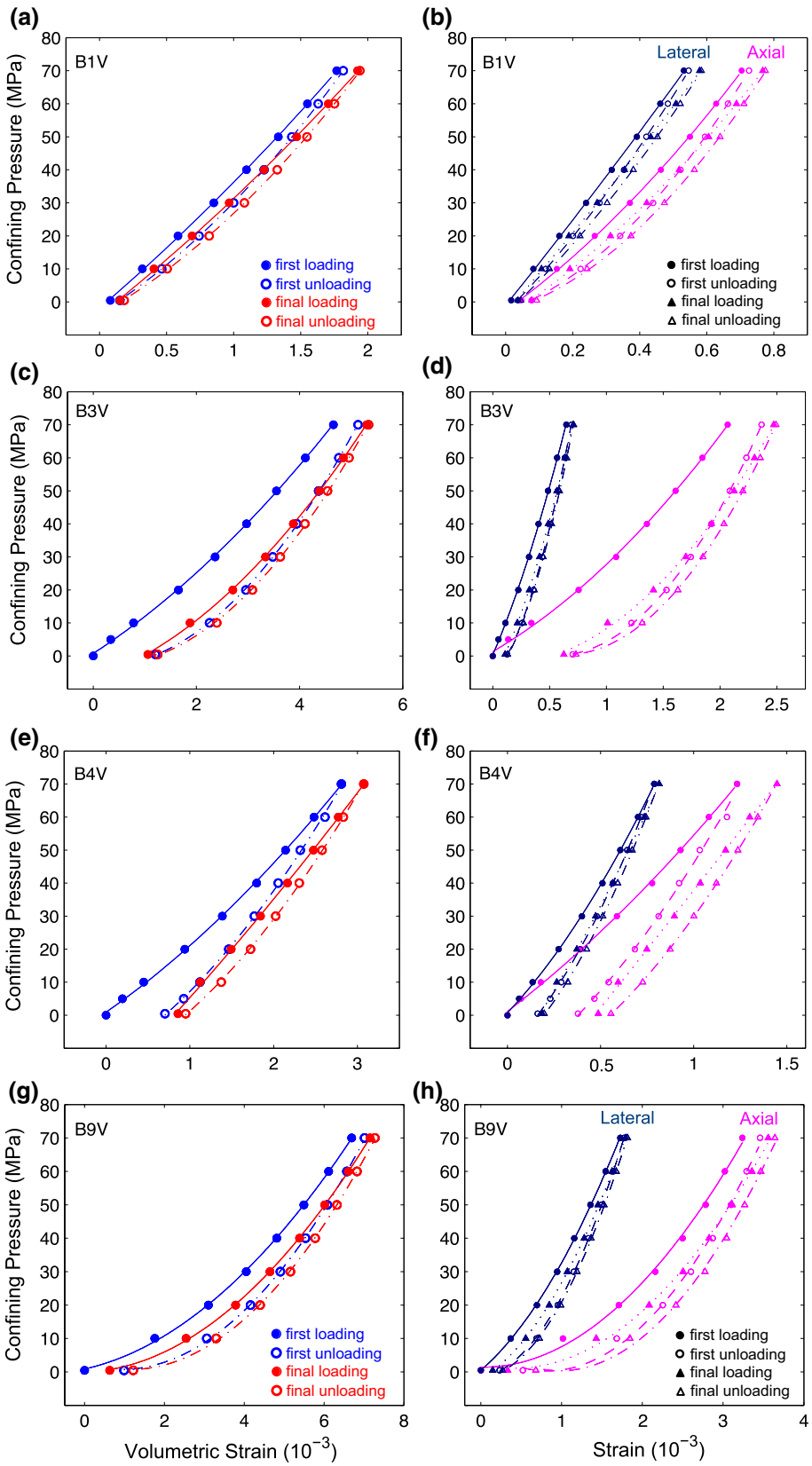

Fig. 4 Confining stress versus strain records of tested specimens during the first and last cycles of seasoning (left column: volumetric strain; right column: axial and lateral strains). Discrete data points are measurements and the curves represent second-order polynomial regressions. The specimen numbers are marked accordingly

Fig. 4 (continued)

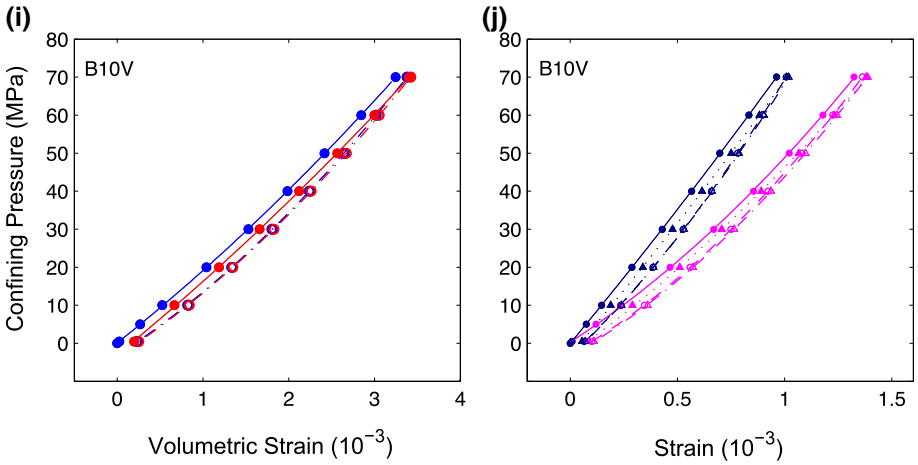

in Specimen B4V (Fig. 5). For the last unloading cycle, both *Vp* and *Vs* nearly coincide with those in the first unloading cycle, a sign that the seasoning is attained.

4 Discussion

The mechanical response of the Bakken specimens is not adequately understood as it is difficult to model their complex microstructure (Bandyopadhyay 2009; Carcione et al. 2011). The presence of compliant components (microcracks, pores and voids) and their interplay with the stress and the microstructure are likely to affect the deformation and wave propagation in an intricate way. Also, all of these factors should be considered under the context of rocks' stress history (in situ conditions and subsequent perturbations). Admittedly, it is only possible to qualitatively build the connection between the mechanical response and the complex microstructure; we would like to comment on several key observations, without assigning much speculation to what actually occurred in these rocks.

4.1 Dependency of stiffness and velocities on confining pressure

The five Bakken specimens show varying degrees of dependency on confinement. Since depths of these cores are within ~ 40 m and the inferred in situ mean stress magnitude does not vary significantly across these sequences, we attribute their contrasts in mechanical response mainly to mineralogical and microstructural differences. In Fig. 6, relationships of confining pressure versus volumetric strain of the last seasoning cycle are summarized for these specimens. It is common that all five cores stiffen as the confining pressure increases, though the stiffness varies significantly from specimen to specimen, and so does the sensitivity of stiffness to confining pressure. It is generally expected that higher compliant component (e.g., clays and kerogen) content contributes to less material stiffness (Vernik and Liu 1997; Sone and Zoback 2013). However, the stiffness does not seem to correlate well with the core's compliant material content. Whether this is affected by measurement error or sample variability is questionable. However, how these compliant components and pore space are distributed throughout the rock matrix and the maturity of the organic matter is critical (e.g., Curtis et al. 2010; Vanorio et al. 2008; Loucks et al. 2009; Sondergeld et al. 2010). A microscopic study of these specimens detailed by Ma and Zoback (2017) revealed that the amount of compliant material content reside between the grains is more important to wave propagation and rock deformation than the total amount residing in the matrix that only occupies the stiff pores. The latter hardly affects the rock matrix stiffness. The surface interactions between the grains and the sandwiched compliant material under increasing confining pressure are particularly relevant.

A summary of wave-propagation velocities of Bakken specimens is presented in Fig. 7. The comparison of velocities between them is generally consistent with the stress–strain response: (1) the stiffness positively correlates with both *P*- and *S*-wave velocities; (2) the sensitivity of velocities to confinement is similar to that of stiffness (except for specimen B10V). We noticed similarities in pressure sensitivity between rocks with similar mineralogies and microstructure. Two fine sandstones, B3V and B9V, exhibited the highest velocities increase with confinement. Two limestone aggregates, B1V and B4V, show moderate velocities dependency on confinement, albeit their initial velocities are quite different. The recrystallized dolomite sediment B10V, different from the two rock types above, only exhibits very limited velocities increase with confinement. Although these specimens show no apparent relationship between compliant material content and stiffness, we are able to find a qualitative correlation between pressure sensitivity of deformation and that of velocities.

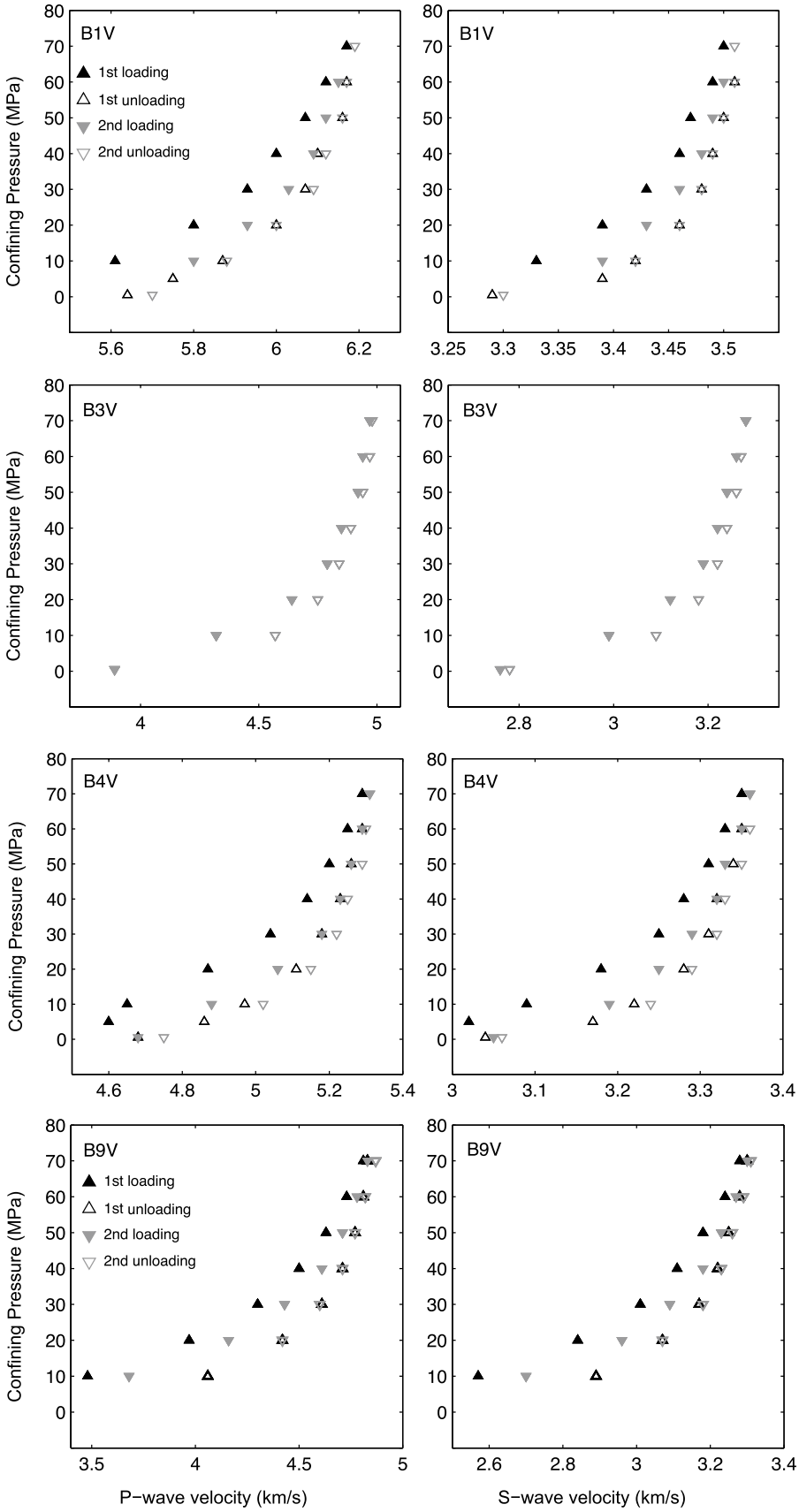

Fig. 5 Confining pressure versus ultrasonic velocity records of tested specimens during the first and last cycles of seasoning. Solid symbols represent loading data and open symbols for unloading data. The specimen numbers are marked accordingly

Fig. 5 (continued)

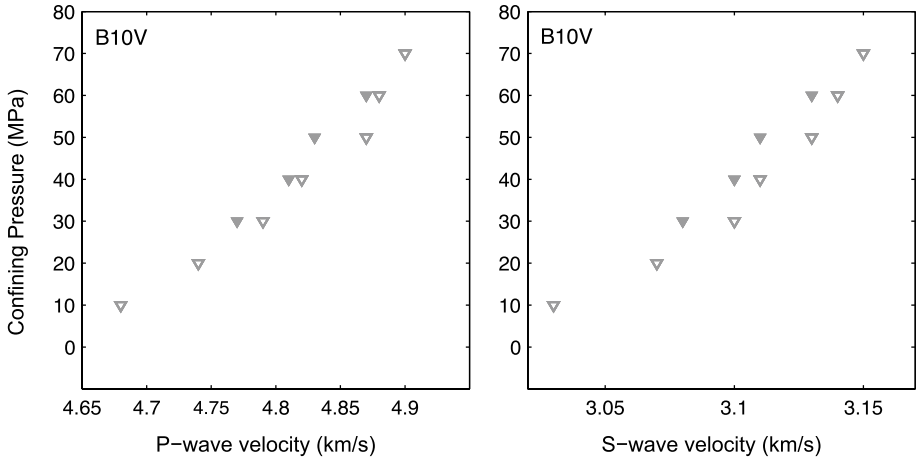

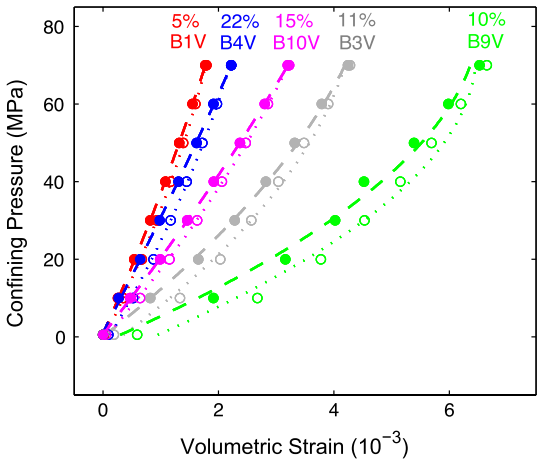

Fig. 6 Confining pressure versus volumetric strain records of five Bakken specimens during the last cycle of seasoning. Discrete data points are measurements (solid circles: loading data; open circles: unloading data), and the curves represent second-order polynomial regressions (dashed lines: loading curves; dotted lines: unloading curves). The specimen numbers are marked accordingly (the percentage indicates the compliant material content)

4.2 Irreversible response between loading and unloading

Appreciable discrepancy in the static and dynamic response between loading and unloading within the first stress cycle is persistent in all specimens tested (Figs. 4, 5). Also, the discrepancy is persistent regardless of confining pressure level (even for confining pressure less than 15 MPa). This discrepancy, often referred to as hysteresis, can be dependent on factors such as inelastic deformation and/or poroelastic effects.

Many processes could introduce inelastic deformation in rocks, and the core extraction is the first step. The extracted core from in situ is known to gradually expand, or de-compact, over time due to stress relief or other effects (Thiercelin and Plumb 1994; Blanton 1983). This expansion is seldom elastic since rock may develop numerous random relaxation microcracks; or rock containing over-pressured fluids may enlarge the pore space or create new 'hydraulic fractures.' In this sense, the rock is intrinsically altered to a new material.

Fig. 7 Confining stress versus ultrasonic velocity records of five Bakken specimens during the last cycle of seasoning. Discrete data points are measurements (solid triangles: loading data; open triangles: unloading data), and the curves represent best-fit regression (dashed lines: loading curves; dotted lines: unloading curves). The specimen numbers are marked accordingly (the percentage indicates the compliant material content)

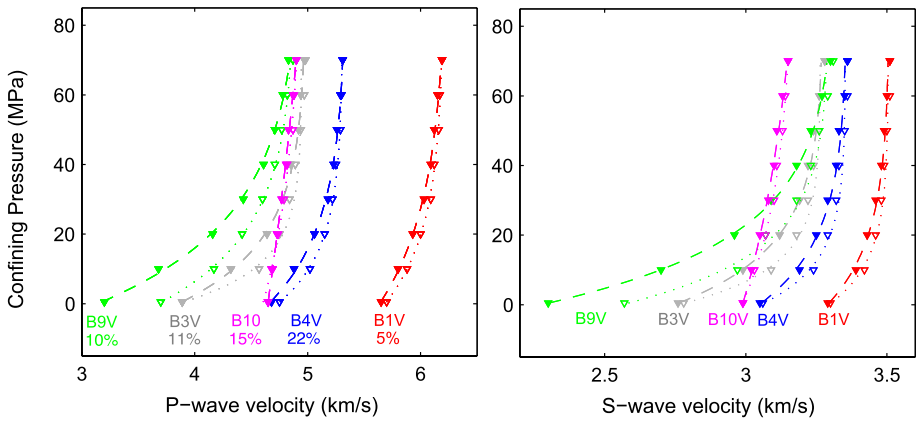

As the expanded core is compacted again in the laboratory, the loading ideally closes the majority of the microcracks/pores and these may not fully re-open during the unloading due to friction or permanent deformation (Scholz and Kranz 1974; Bernabé 1986; Jæger et al. 2007). The influence of compliant component presence is another possible explanation for the hysteresis we observed. The inelastic compaction upon loading and rebound upon unloading can also contribute to such discrepancy. The extent of such discrepancy varies from rock to rock, as it is apparently related to the rock's intrinsic lithofacies and external perturbations (e.g., stress history).

The poroelastic effects due to the remaining fluid content cannot be overlooked when the core is loaded/unloaded instantaneously. The poroelastic effect would manifest itself as a time-dependent process that affects the deformation of the specimen. We did observe time-dependent deformation in these cores; however, the time-dependent deformation under constant stress is significantly smaller than the instantaneous deformation caused by stress loading/unloading (for details, see Ma and Zoback 2017). In addition, it is important to note that these reservoir rocks also deform in a time-dependent manner (viscous) (regardless of being elastic or inelastic) (Sone and Zoback 2013), since they contain certain amounts of compliant components (e.g., clays and kerogen). The extent to which poroelastic effect and viscoelastic/plastic effect contribute is unclear. Therefore, their effect on the hysteresis is of questionable significance.

Last but not the least, the hysteresis could be induced by imperfect placement/alignment and conditioning of the specimen with respect to the loading apparatus and the deformation/velocity sensors. This is an issue typically comes with experimentation but may diminish with the number of loading cycles. It is difficult to distinguish this from the hysteresis inherent to the specimen, but its effect is certainly not to be overlooked.

4.3 Evolution with Multiple Cycles

The purpose of subjecting the rock to multiple pressure cycles is to minimize the aforementioned influences and to yield a specimen with reproducible response. What we observed in the seasoning process is that: (1) the discrepancy between the loading and unloading in the final cycle is significantly reduced as compared to the first cycle and (2) the final unloading curve resembles the first unloading curve, although there is typically an offset between the two. Apparently, each time the specimen is re-loaded to the maximum stress applied, certain amount of inelastic deformation is induced, which essentially causes the discrepancy between the unloading curve and its neighboring loading curves. This poses the question that whether the specimen is being cycled toward its intrinsic response in situ or being continuously altered into a new material.

Many studies have shown that cyclic loading may gradually damage the rock (e.g., Haimson 1974; Zoback and Byerlee 1975; Rao and Ramana 1992; Heap and Faulkner 2008; Heap et al. 2009a, b; Wang et al. 2013). In these studies, the differential stress between axial stress and confining pressure was cycled, which induces cycled shear stress and corresponding distortion that facilitates the development of microcracks. In our seasoning process, only hydrostatic loading is applied. Although some rocks may fail or damage significantly even just under hydrostatic loading study (such as porous sandstones reported by Zhang et al. (1990)), it is important to note that if the cycled hydrostatic loading is not sufficiently high to cause damage, seasoning should merely close microcracks and compact compliant materials. Nonetheless, we are cognizant that hydrostatic stress cycles at only moderate levels may cause damage to rocks due to several mechanisms. First is that the material may fatigue due to subcritical crack growth (e.g., Heap et al. 2009a, b), irreversible compaction of compliant component, or other forms of time-dependent degradation. Secondly, the Bakken specimens are laminated materials and highly anisotropic in mechanical properties (Fig. 4). The hydrostatic stress in one principal direction might be moderate but might exceed the threshold of inducing additional damage in other principal directions.

5 Concluding Remarks

We have conducted a suite of hydrostatic compression tests in five bedding-perpendicular cores from the Bakken formation. The objective was to characterize the static and dynamic response of these cores and to understand the effectiveness of seasoning on them. The measurements revealed a strong pressure dependency in all Bakken cores. Both the static (deformation) and dynamic (wave propagation) responses show the stiffness of these specimens increases with confining pressure, albeit at a decreasing rate. Hysteresis between loading and unloading was observed in all cycles, but it diminishes with the number of cycles. Strain measurements suggest the hysteresis is mainly attributed to axial inelastic deformation for these anisotropic rocks, and the velocity measurements in the axial direction consistently show hysteretic behavior.

The comparison of mechanical response between five Bakken cores revealed their differences in stiffness, which is characteristic of the core mineralogies and microstructures. Although we typically expect the content of soft components (clays and kerogen) positively correlates with the rock's compliance, it is not necessarily the case for these Bakken cores. The correlation is perhaps highly dependent

on how the soft components are distributed and aligned in the matrix. Further study is warranted with microscopic imaging and analysis.

The evolution of mechanical response with cycles suggests it is possible to obtain reproducible measurements after seasoning. Apparently seasoning reduces uncertainties and variability in the experiments. But it is not clear whether seasoned rock is representative of the material in situ or deviates more from it. The effect of seasoning could: (1) close (or extend) stress-relief microcracks and (2) compact soft components. Whether the rock has been further altered by seasoning is subject to the applied confinement as compared to its in situ stress condition and its material properties. To conclude, seasoning is not a remedy for restoring rock's intrinsic behaviors, but it could certainly provide meaningful insights into understanding better the rock's response subject to human perturbation and re-conditioning.

Acknowledgements This work was supported by the Stanford Rock Physics and Borehole Geophysics Project (SRB) and the Open Research Fund of the State Key Laboratory of Geomechanics and Geotechnical Engineering, Institute of Rock and Soil Mechanics, Chinese Academy of Sciences (Grant No. Z015002). The Bakken cores tested in this study were kindly provided by the Hess Corporation. We thank the associate editor and two anonymous reviewers for their comments that greatly helped improve this contribution.

References

Bandyopadhyay K (2009) Seismic anisotropy: geological causes and its implications to reservoir geophysics. Ph.D. thesis, Stanford University

Bernabé Y (1986) The effective pressure law for permeability in Chelmsford granite and Barre granite. Int J Rock Mech Min Sci 23(3):267–275

Blanton TL (1983) The relation between recovery deformation and in situ stress magnitudes. SPE/DOE-11624. Symposium on Low Permeability, Denver, Colorado, 14–16 March 1983

Boutéca MJ, Bary D, Fourmaintraux D (1998) Does the seasoning procedure lead to intrinsic properties? SPE/ISRM Eurock'98, Trondheim

Carcione JM, Helle HB, Avseth P (2011) Source-rock seismic-velocity models: Gassmann versus Backus. Geophysics 76(5):N37–N45. https://doi.org/10.1190/geo2010-0258.1

Curtis ME, Ambrose RJ, Sondergeld CH, Rai CS (2010) Structural characterization of gas shales on the micro- and nano-scales. Presented at Canadian Unconventional Resources and International Petroleum Conference, CUSG/SPE 137693

Dewhurst DN, Siggins AF (2006) Impact of fabric, microcracks and stress field on shale anisotropy. Geophys J Int 165(1):135–148. https://doi.org/10.1111/j.1365-246X.2006.02834.x

Dewhurst DN, Sarout J, Delle Piane C, Siggins AF, Raven MD (2015) Empirical strength prediction for preserved shales. Mar Pet Geol 67:512–525. https://doi.org/10.1016/j.marpetgeo.2015.06.004

Dohmen T, Blangy J-P, Zhang J (2014) Microseismic depletion delineation. Interpretation 2:SG1–SG13

Ewy R (2015) Shale/claystone response to air and liquid exposure, and implications for handling, sampling and testing. Int J Rock Mech Min Sci 80:388–401

Haimson BC (1974) Mechanical behavior of rock under cyclic loading. In: Advances in rock mechanics, vol 2, part 1. National Academy of Sciences, Washington

Heap MJ, Faulkner D (2008) Quantifying the evolution of static elastic properties as crystalline rock approaches failure. Int J Rock Mech Min Sci 45:564–573

Heap MJ, Vinciguerra S, Meredith PG (2009a) The evolution of elastic moduli with increasing crack damage during cyclic stressing of a basalt from Mt. Etna volcano. Tectonophysics 471:153–160

Heap MJ, Baud P, Meredith PG, Bell AF, Main IG (2009b) Time-dependent brittle creep in Darley Dale sandstone. J Geophys Res 114:B07203

Hornby BE (1998) Experimental laboratory determination of the dynamic elastic properties of wet, drained shales. J Geophys Res 103(B12):29945–29964. https://doi.org/10.1029/97JB02380

Hornby BE, Schwartz LM, Hudson JA (1994) Anisotropic effective-medium modeling of the elastic properties of shales. Geophysics 59:1570–1583. https://doi.org/10.1190/1.1443546

Jæger CJ, Cook NGW, Zimmerman R (2007) Fundamentals of rock mechanics, 4th edn. Wiley-Blackwell, Hoboken

Johnston JE, Christensen NI (1995) Seismic anisotropy of shales. J Geophys Res 100:5991–6003. https://doi.org/10.1029/95JB00031

Josh M, Esteban L, Delle Piane C, Sarout J, Dewhurst DN, Clennell MB (2012) Laboratory characterisation of shale properties. J Pet Sci Eng 88–89:107–124. https://doi.org/10.1016/j.petrol.2012.01.023

Loucks RG, Reed RM, Ruppel SC, Jarvie DM (2009) Morphology, genesis, and distribution of nanometer-scale pores in siliceous mudstones of the Mississippian Barnett Shale. J Sediment Res 79:848–861. https://doi.org/10.2110/jsr.2009.092

Ma X, Zoback M (2016a) Laboratory investigation on effective stress in Middle Bakken: implications on poroelastic stress changes due to depletion and injection. ARMA 16-48 presented at 50th U.S. Rock Mechanics Geomechanics Symposium, Houston, 26–29 June 2016

Ma X, Zoback M (2016b) Experimental study of dynamic effective stress coefficient for ultrasonic velocities of Bakken cores. SEG International Exposition and 86th Annual Meeting, Dallas, 16–21 October 2016

Ma X, Zoback M (2017) Laboratory experiments simulating poroelastic stress changes associated with depletion and injection in low-porosity sedimentary rocks. J Geophys Res Solid Earth. https://doi.org/10.1002/2016JB013668

Mavko G, Mukerji T, Dvorkin J (2009) The rock physics handbook, 2nd edn. Cambridge University Press, Cambridge

Ostermeier (1995) Deepwater gulf of mexico turbidites-compaction effects on porosity and permeability. SPE Formation Evaluation, pp 79–85

Pham QT, Vales F, Malinsky L, Nguyen Minh D, Gharabi H (2005) Effect of desaturation-resaturation on mechanical behavior of shale. The 40th U.S. Symposium on Rock Mechanics (ARMA/USRMS 05-793) held in Anchorage, Alaska, 25–29 June 2005

Rao MVMS, Ramana YV (1992) A study of progressive failure of rock under cyclic loading by ultrasonic and AE monitoring techniques. Rock Mech Rock Eng 25:237–251

Santarelli FJ, Dusseault MB (1991) Core quality control in petroleum engineering. In: Roegiers JC (ed) Rock mechanics as a multidisciplinary science. Balkema, Rotterdam

Sarout J, Guéguen Y (2008) Anisotropy of elastic wave velocities in deformed shales: part 1—experimental results. Geophysics 73(5):D75–D89. https://doi.org/10.1190/1.2952744

Sarout J, Esteban L, Delle Piane C, Maney B, Dewhurst DN (2014) Elastic anisotropy of Opalinus Clay under variable saturation and triaxial stress. Geophys J Int 198:1662–1682. https://doi.org/10.1093/gji/ggu231

Scholz CH, Kranz R (1974) Notes on dilatancy recovery. J Geophys Res 79:2132–2135

Sondergeld CH, Rai CS (2011) Elastic anisotropy of shales. Lead Edge 30:324–331. https://doi.org/10.1190/1.3567264

Sondergeld CH, Rai CS, Margesson RW, Whidden KJ (2000) Ultrasonic measurement of anisotropy on the Kimmeridge shale. In: 70th Annual International Meeting, SEG, Expanded Abstracts, pp 1858–1861

Sondergeld CH, Ambrose RJ, Rai CS, Moncrieff J (2010) Microstructural studies of gas shales. Presented at SPE Unconventional Gas Conference, SPE 131771

Sone H, Zoback MD (2013) Mechanical properties of shale-gas reservoir rocks—part 1: static and dynamic elastic properties and anisotropy. Geophysics 78(5):D381–D392

Thiercelin MJ, Plumb RA (1994) Core-based prediction of lithologic stress contrasts in East Texas formations. SPE Formation Evaluation

Vanorio T, Mukerji T, Mavko G (2008) Emerging methodologies to characterize the rock physics properties of organic-rich shales. Lead Edge 27:780–787. https://doi.org/10.1190/1.2944163

Vernik L, Liu X (1997) Velocity anisotropy in shales: a petrophyscial study. Geophysics 62:521–532. https://doi.org/10.1190/1.1444162

Vernik L, Milovac J (2011) Rock physics of organic shales. Lead Edge 30:318–323. https://doi.org/10.1190/1.3567263

Vernik L, Nur A (1992) Ultrasonic velocity and anisotropy of hydrocarbon source rocks. Geophysics 57:727–735. https://doi.org/10.1190/1.1443286

Wang HF, Simmons G (1978) Microcracks in crystalline rock from 5.3-km depth in the Michigan Basin. J Geophys Res 83(B12):5849–5856

Wang Z, Li S, Qiao L, Zhao J (2013) Fatigue behavior of granite subjected to cyclic loading under triaxial compression condition. Rock Mech Rock Eng 46(6):1603–1615

Warpinski NR, Teufel LW (1992) Determination of the effective stress law for permeability and deformation in low-permeability rocks. SPE Formation Evaluation. No. 20572, pp 123–131

Yang Y, Zoback MD (2014) The role of preexisting fractures and faults during multistage hydraulic fracturing in the Bakken formation. Interpretation 2:SG25–SG39

Zhang J, Wong T-F, Davis DM (1990) Micromechanics of pressure-induced grain crushing in porous rocks. J Geophys Res 95(B1):341–352

Zoback MD, Byerlee JD (1975) The effect of cyclic differential stress on dilatancy in Westerly granite under uniaxial and triaxial conditions. J Geophys Res 80(11):1526–1530